A Study of Small-Scale Energy Networks of the Japanese Syowa Base in Antarctica by Distributed Engine Generators

Shin'ya OBARA
Kitami Institute of Technology, Power Engineering Lab., Dep. of Electrical and Electronic Engineering
Koen-cho 165, Kitami, Hokkaido 090-8507, Japan
obara@mail.kitami-it.ac.jp
phone/FAX +81-157-26-9262

Yuta MORIZANE
Kitami Institute of Technology, Power Engineering Lab., Dep. of Electrical and Electronic Engineering
Koen-cho 165, Kitami, Hokkaido 090-8507, Japan

Abstract

Fuel traffic to the Syowa Base of the South Pole is increasing from Japan, with growing research and observation occurring every year. Limits to fuel traffic and the spread of green energy utilization are topics of interest for Syowa Base; this research considers the construction of a Syowa Base small-scale energy network (Syowa Base Micro-Grid: SBMG) for the purposes of reducing fuel consumption and increasing green energy utilization. The number of engine generators, the operation plan for the battery's charge and discharge, and the introduction of an exhaust heat pump provided a means by which the load factor of the engine generator could be maintained high value from the fluctuations of green energy. This might be accomplished by modifying the main power supply of Syowa Base into a distributed power supply system rather than a conventional central power supply system. The relationship between the amount of green energy (photovoltaics and wind power generation) connected to the proposed power supply distribution and the amount of fuel consumed by the engine generators and backup boiler was clarified. Moreover, the outside temperatures, insulation levels, and wind velocity at the Syowa Base change seasonally, resulting in large changes in the SBMG operation method. Therefore, differences in the operation methods between the proposed power supply distribution system and the conventional central power supply were assessed during the summer

(January), winter (July), and mid-season (October), and the resulting differences in fuel consumption were clarified.

Key Words: Antarctic Pole, Local Energy, Microgrid, Green Energy, Photovoltaics, Wind Power Generation

1. Introduction

Syowa Base was established as a Japanese observation base in an area of the South Pole known as East Ongul in 1957. Syowa Base is the base camp for the Mizuho base, the Asuka observation base, and the Dome Fuji observation base. The energy used by Syowa Base comes from fuel transported by the observatory ship Shirase on a yearly basis; this fuel represents 50 to 60% of the total cargo shipment of Shirase. The amount of fuel consumption is increasing as the research and observations conducted at the South Pole increase. For this reason, energy conservation, the restriction of the cargo shipment fuel quantities brought by Shirase, and a shift to clean energy at Syowa Base are all important subjects. The introduction of photovoltaics and wind power generation has been attempted at Syowa Base [1]. The main (central) power supply of Syowa Base is a 240-kW diesel engine generator. It will become necessary to increase the level of green energy sharply in response to a reduction in fuel transport volume, especially given the negative environmental impact of the exhaust gases [1, 2]. When unstable green energy is connected with a small-scale independent power network, this causes subsequent problems in the quality of the power supply in terms of voltage and frequency. The power network of Syowa Base therefore requires a plan to address the unstable nature of the electric power supplied through green energy sources. Moreover, Syowa Base requires a large amount of heat for its heating, hot-water supply, and thawed drinking water [1, 2]. The heat demand has exceeded the electricity demand, such that at present, Syowa Base is supplied with heat via engine exhaust and the combustion of fossil fuel. Generally, the voltage and frequency of a power network driven by green energy can be divided into fluctuations of a short duration and fluctuations of a long duration. Short-term fluctuations are controllable using a grid connection to a power conditioner, a battery, and a STATCOM (static synchronous compensator). In contrast, longer fluctuations are controlled through the partial load operation of an engine generator or a large-scale storage battery. However, there is a minimum in the load factor of an engine generator, and the power generation efficiency with small

loads therefore suffers. The output ratio of exhaust heat increases with decreases in the power generation efficiency at the time of low loads. Due to the high level of heat demand at Syowa Base, decreases in the power generation efficiency of the engine generator will not become a significant problem. However, in terms of the introduction of an electric heat pump to reduce the fuel required for heating, to control the amount of harmful exhaust gas discharge, and to generate a heat supply using green energy, a high power generation efficiency is advantageous. To obtain a high power generation efficiency, it is necessary to maintain a high load factor for the engine generator. Two or more small engine generators are therefore linked as the main power supply of Syowa Base; this paper considers the control method for their operation. Below, the method of linking two or more small engine generators and controlling the operations described above is described in terms of a distributed power supply system [3-8]. Because the distributed power supply system can control the number of engine generator operations to address long-term fluctuations in the green energy supply, the loading factor of the operating engine generators is kept at a high level. Because the power generation efficiency of this system is high, the operation of an electric heat pump is advantageous. In the current energy system of Syowa Base, engine exhaust heat provides heat for a heating medium (antifreeze solution) via a heat exchanger. This heat medium is then supplied to the demand side using a circulating pump. The heat medium heats each building before returning to an exhaust heat exchanger. In the proposed system, the heat pump would be installed in the middle of the demand side. Therefore, because the heat source temperature of the heat pump is sufficiently higher than the outside temperature, a high COP (coefficient of performance) is maintainable. By updating the main power supply to the distributed power supply system, which controls the number of engine generator operations from a conventional central power supply system, and by introducing a heat pump using the exhaust heat, increases in the level of green energy available to this small-scale energy network (Syowa Base Micro-Grid: SBMG) and a reduction in fuel consumption may be achievable.

2. The Energy System and Climate Conditions of Syowa Base

2.1 Conventional Energy System of Syowa Base

Locations beyond the 70 main buildings (in an area covering 6981 m^2), such as a water storage tank, various antennas, and oil storage tanks, are also included at Syowa Base. Figure 1 shows the arrangement of the buildings of Syowa Base in 2011 and provides an outline of the electric power and

heat equipment. Accommodation spaces, such as an administration building (A_4 in Fig. 1), three power generation buildings (A_0, B_0, H_2), two residence buildings (A_1, A_2), 19 observation and research buildings, four warehouses, and one garage, are shown as they appeared in 1991. Heat for space heating and hot-water supply is currently supplied from the exhaust heat of an engine generator, electric heaters, kerosene boilers, oil-based stoves, and a solar collector. The main power supply is a 240 kW diesel engine generator, which is also the central power supply. The diesel engine generator is linked to each building and all photovoltaics (E_0, 55 kW) of the base through the SBMG. Diesel engine generators are installed in the electricity-production building (A_0), in a storage and sewage disposal building (A_3), in an administration building (A_4), and in two residence buildings (A_1, A_2), and these buildings are therefore heated via engine exhaust. The solar collector, the electric heaters, the kerosene boilers and the oil-based stoves are used to heat and provide hot water to the other buildings. Table 1 shows the annual fuel consumption of Syowa Base. The fuel required for power generation is 430 kL, and the fuel required for space heating is 87 kL [1 and 2]. This research examines an energy system designed to reduce the total amount of fuel (430 kL) for power generation and heating (87 kL), as described above.

2.2 A Future Model for the Syowa Base Micro-Grid

Figure 2 (a) depicts a model of the future SBMG of Syowa Base, as proposed in this research. Two or more combinations (Figure 2 (b)) of a small engine generator, a heat storage tank, and a heat pump are introduced into the power generation building (A_0; the distributed power supply system) in the future SBMG. In the area near the engine generators, such as the electricity-production building, storage and sewage disposal building, administration building, and residence buildings, heat is provided by engine exhaust heat, a heat pump, and a backup boiler. Power is supplied to the power network by linking each supply source to the diesel engine generators, photovoltaics (E_0), and wind power (E_1), described above. With the exception of the ridges described above and the green energy building (F_1), an electric storage heater (Fig. 2 (c)) is installed in each ridge in the future SBMG model. Each building of the base can thus be heated simply and safely through the introduction of an electric storage heater. Furthermore, the load factor of the engine generatorsould be highly controllable by using electricity from storage heaters. As a result, the power generation efficiency of the engine generator is highly maintainable. With the introduction of electric storage heaters, the stabilization of green energy

(photovoltaics and wind power) fluctuations and the management of the heating of all the ridges from within the control room of the administration building could be accomplished.

2.3 Outline of the SBMG with the Distributed Power Supply

The effects of introducing green energy to the SBMG when changing the current central power supply installed in the energy-production building (A_0) to a distributed power supply are considered. An engine generator for the main power supply distributes and arranges three sets within the energy-production building (A_0) and links them to the SBMG using photovoltaics (E_0) and wind power (E_1). The introduction of an electric storage heater, described in Figs. 2 (a) and (c), is not taken into consideration for the purposes of this paper. Space heating, hot-water supply, and thawed drinking water for the residence building, the administration building, the electricity-production building, the storage building, and the sewage disposal building (from A_0 to A_4), which are the main facilities responsible for maintaining staff life, are supplied via exhaust heat from engine generators, heat pumps, and backup boilers. Space heating of other buildings is usually accomplished via electric heaters, kerosene boilers, oil-based stoves, and a solar collector. Therefore, to provide the details of the electric power load and heat load used in following analysis, the records of the previous conventional energy system (Fig. 1) are used. Future plans for an SBMG serving the whole base for space heating each building, the possible effects of improving the efficiency of the engine generators, and the means to stabilize green energy using an electric storage heater are described in the following report.

2.4 Weather Conditions and Fuel Consumption

Figure 3 shows the meteorological data, including temperature, wind velocity, and insulation level, as measured on Syowa Base [1, 2, 10]. Figure 3 (a) shows the average outside temperature in January (summer), July (winter), and October (mid-season) at Syowa Base (from 2009 to 2010). Although daytime temperatures are somewhat higher than nighttime temperatures in January and October, given the lack of solar radiation, the differences in daytime and nighttime temperature in July are small. Figure 3 (b) shows the average wind velocity for each sampling time on a representative day of every month. Fluctuations in the average monthly wind velocity are large from 6:00 to 13:00, and in the summer (January), the fluctuation is larger than in the winter (July). Moreover, Figure 3 (c) shows the average solar radiation at each sampling point measured on a representative day of every month. The

150 solar radiation at Syowa Base is greatest during the summer, and there is no solar radiation during the
151 winter. A total of 55 kW of photovoltaics are linked to the power network of Syowa Base, and a
152 maximum production of 52.5 kW of electricity was recorded during December of 2010 [9]. From the
153 data shown (Fig. 3), the amount of space heating required by Syowa Base and the amount of green
154 energy (wind power and photovoltaics) available differs greatly by month.
155 The fuel used by Syowa Base (shown in Table 1) is transported to the base from Japan by the
156 observatory ship Shirase once per year. With the central power supply currently used by the
157 conventional SBMG shown in Fig. 1, 430 kL of diesel fuel is consumed each year. The diesel engine
158 generators being used in cogeneration and space heating and to provide the hot-water supply and
159 thawed drinking water for the residence building, administration building, power generation building,
160 storage building, and sewage disposal building (A_0 to A_4; excluding the electricity demand for the
161 whole Syowa Base) are included in this 430 kL requirement. Furthermore, 87 kL of JP-5 fuel is used
162 every year for space heating the additional buildings and facilities.
163
164 ## 3. Planning the Syowa Base Microgrid
165 ### 3.1 The Energy Demand Characteristics of Syowa Base
166 The measurements in Fig. 4 (a) show the average, minimum, and maximum monthly power load,
167 whereas the measurement in Fig. 4. (b) shows the monthly electricity production of the engine
168 generator and photovoltaics (PV) [2]. From Fig. 4 (a), the maximum of the power load in one year is
169 1.71 times the minimum power load and is accompanied by an average fluctuation of approximately
170 20%. The current production of electricity from the PV is very small for the engine generator, as shown
171 in Fig. 4 (b), but an expansion in the amount of PV and wind power is planned for the future [9]. Figure
172 5 shows the amount of power from engine exhaust heat required in summer, winter, and mid-season
173 and the heat supply calculated from the fuel consumption of boilers and heaters for space heating. The
174 exhaust heat supplied by the engine generator is 86% of the summer heat demand, and 51% of the
175 winter heat demand.
176
177 ### 3.2 The Central Power Supply and the Distributed Power Supply
178 Figure 6 (a) shows the rate of fuel consumption for various types of distributed power supply systems
179 with respect to the central power supply system. The engine generator used in Fig. 6 (a) is a

combination of commercial items [11]. The fuel consumption required to power one set of 309 kW engine generators ((A) in the figure) is set to 100% in Fig. 6 (a). In contrast, "(B) to (E)" in the figure refer to the fuel consumption characteristics when the engine generators of two or more small-capacity systems are combined (distributed power supply is assumed). Moreover, yellow areas in the figure show the range of annual power loads at Syowa Base. As shown in Fig. 6 (a), the fuel consumption of the partial load operations with the distributed power supply system is advantageous for a central power supply system. Because the maximum power generation efficiency increases when the capacity of an engine generator is large, increases in the number of engine generators lead to a decrease in the power generation efficiency of the maximum load. Therefore, it is necessary to plan the number of engine generators appropriately based on the power generation efficiency of the whole system. Figure 6 (b) shows the characteristics of the load factor, the power generation efficiency and the heat power efficiency of the central power supply system (240 kW) currently installed at Syowa Base, and the distributed power supply system (113 kW, three sets) assumed in this paper. Although the maximum efficiency of the 240 kW engine generator is higher than that of the 113 kW engine generator, when the same load factor is measured in Fig. 6 (b), there is more exhaust heat produced by the 113 kW engine generator.

3.3 The Syowa Base Microgrid

Figure 7 shows the proposed SBMG considered here. The composition group of an engine generator, a heat storage tank, a heat pump, a backup boiler in three sets (Power unit A, B, C), and an electric storage heater are not considered in the following analysis. The energy system of the existing Syowa Base is modified into a distributed power supply system from a central power supply, and the supply capability through photovoltaics and wind power generation is thereby increased. A heat supply system, a heat storage tank, an electric heat pump, and a backup boiler are installed in the exhaust heat circulation system of the engine generator. Therefore, the low-temperature side of the heat pump's heat source is the engine exhaust heat, after supplying heat to the demand side. Engine exhaust heat exchanges heat with a heating medium (such as antifreeze solution, used here) in an exhaust heat exchanger, and this heating medium is then directly supplied to the demand side. When engine exhaust heat is used as the heat source for low-temperature heat pumps, the heat source temperature is stabilized compared with the open air, and high coefficients of performance are expected. However,

because the capacity of the heat pump is restricted to the amount of engine exhaust heat, the introduction of backup boilers B_0, B_1, and B_2 are shown (Fig. 7) after the introduction of a heat pump is assumed in the following analysis model. The electric power supply to the electric heat storage heater can be supplied in two ways: via a green-energy system (with an electricity power network for heating) and via an electric power system with green energy (and an electricity power network). The electric power supplied to the electric heat storage heater has a wide allowable width of voltage fluctuations and frequencies compared with the electric power system used in equipment observation and in household appliances. Therefore, green energy with significant fluctuations can be used to power an electric storage heater. In contrast, when the heat load cannot be provided to the electric storage heater by green energy, the engine generator can receive power support from the electric power system. Many functions can be controlled through a management office using a control line, including start and stop functions, power adjustments, measurements of the network frequency and voltage, the power supplied to an electric storage heater, power adjustments of the heat pump, a temperature survey of warm-water circulation for space heating (heat medium), power measurements of green energy, and operation and control of the wind power.

As Section 2.3 described, the analysis presented in this paper does not consider the introduction of an electric storage heater. Moreover, the number of installed engine generators with a heat pump, a heat storage tank, and a backup boiler may be modified from Fig. 7 according to the results of the operation analysis described in Chapter 5.

3.4 The Operation Method of the Engine Generator

Figure 8 shows an outline of the operation method of distributed engine generators installed in the SBMG. Fig. 8 (a) shows the electric power load pattern of Syowa Base on a representative day, and green energy (PV and aerogenerator) power patterns are shown in Fig. 8 (b), along with three sets of engine generators with the same capacity; E/G0, E/G1, and E/G2 transmit electricity according to the same power load pattern. Therefore, the power load (Fig. 8 (c)) of the engine generators is the value excluding the green energy (Fig. 8 (b)) of the power load (Fig. 8 (a)) for the whole base. Three sets of engine generators control the operations according to the magnitude of the load. When the electric power load is changed, an increase in operation times because of the low power generation efficiency caused by partial loads will occur frequently. Moreover, when the load factor of the engine generator is

small, maintaining stable operations generally becomes difficult. Therefore, the minimum load factor of the engine generators due to the distributed power supply system is set to 50%, and the engine generator is operated by outputs of 0% (neutral operation), 50%, or 100%. When the output of the engine generator is set at 0 %, 50 %, or 100 %, the timing of the surpluses and shortages in the supply-and-demand balance of electric power occurs as shown in Fig. 8 (d). The load follow-up control of the engine generator is not adopted by the engine operating life in this system. The supply-and-demand balance of electric power can be adjusted through the charging and discharging of a battery, as shown in Fig. 8 (d). As a result, the output of each engine generator can obtain a high load factor in many time zones, as shown in Fig. 8 (e). Because E/G2 does not work in the example of Fig. 8 (e), one set of the engine generators is unnecessary.

3.5 The Heat Pump Operation Method

Figure 9 is a block diagram of the heat engine and the heat pump to be introduced into the SBMG. The calorific value $h_{1,i,t}$ of the fuel outputs external work $l_{eg,i,t}$ and exhaust heat $h_{2,i,t}$. When $l_{eg,i,t}$ is given to the power generator (G/Ti) with a power generation efficiency $\eta_{gt,i}$, the electric power $e_{gt,i,t}$ will be outputted to the power network. The electric power $e_{pv,t}$ of PV and the electric power $e_{wp,t}$ of wind power generation other than $e_{gt,i,t}$ link to the power network. In contrast, electric power is consumed by the electric power load $e_{pst,t}$ in the base, and the electric power load $e_{mt,i,t}$ of the heat pump. Numbers in red in Power unit A of Fig. 9 indicate the distribution of energy based on the calorific value ($h_{1,i,t}$) of fuel with an engine generator operating at maximum efficiency. When the efficiency $\eta_{gt,i}$ of a power generator is 0.9, the efficiency $\eta_{mt,i}$ of the motor of the heat pump is 0.9, and the COP is set to 4.0. Furthermore, the total mechanical loss of the engine generator and radiation-based heat loss of the engine, heat storage tank, piping, etc., is set (according to past records of a real system) to 11% of the fuel calorific value. Heat demand is divided into Heat demand A and Heat demand B (in the case of $i = 0$) in the figure; a portion of the engine exhaust heat $h_{2,i,t}$ is supplied to Heat demand A, and the sum total of heat $h_{5,i,t}$ from heat pump and backup boiler $h_{5,i,t}$ is supplied to Heat demand B. When not taking into consideration the electric power supply to the power network by green energy, the maximum output of the heat pump is 34.5% of the fuel calorific value $h_{1,i,t}$. The output of the heat pump $h_{w2,i,t}$ is the sum of the quantity of the heat $h_{4,i,t}$ from a heat source at low temperatures and the output of an electric motor $l_{mt,i,t}$. Therefore, although a large

amount of electric power from green energy is supplied to the heat pump, the output of heat pump $h_{w2,i,t}$ is restricted by the magnitude of $h_{4,i,t}$.

3.6 Energy balance equations

Equation (1) is an energy balance equation of the electric power in sampling time t of the SBMG shown in Fig. 2. The left side of Eq. (1) is the output power item and the right side is the consumption power item. The output e_{pv} of the photovoltaics of the N_{pvu} set, output e_{wp} of wind power generation of the N_{wpu} set, output e_{eg} of the engine generators of the N_{eg} set, and the input/output of battery e_{bt} are the supply terms for the transmission network of electric power. In contrast, electric power is consumed by the electricity demand Δe_{load} of the right-hand side of Eq. (1): power consumption Δe_{hp} of a heat pump of the N_{eg} set, power consumption Δe_{esh} of an electric heat storage heater of the N_{esh} set, and loss Δe_{loss}. Loss of a power conditioner for PV, loss of power generators, and the charge/discharge efficiency of the battery are included in Δe_{loss}.

$$\sum_{i=1}^{N_{pvu}} e_{pv,i} + \sum_{j=1}^{N_{wpu}} e_{wp,j} + \sum_{k=1}^{N_{eg}} e_{eg.k} + e_{bt} = \Delta e_{load} + \sum_{m=1}^{N_{eg}} \Delta e_{hp,m} + \sum_{n=1}^{N_{esh}} \Delta e_{esh,n} + \Delta e_{loss} \quad (1)$$

Next, Eq. (2) is the heat balance equation at sampling time t of the SBMG. The left-hand side of Eq. (2) is the output term of heat, and the right-hand side is the input term of the heat load. Heat is supplied to the heat load Δh_{load} of the N_{loadh} set from thermal power h_{eg} of engine generators of the N_{eg} set, thermal power h_{esh} of the electric heat storage heater of the N_{esh} set, thermal power h_{hp} and h_{bo} of the heat pump and backup boiler of the N_{eg} set, and the input/output h_{hst} of the heat storage tank of the N_{eg} set.

$$\sum_{k=1}^{N_{eg}} h_{eg,k} + \sum_{n=1}^{N_{esh}} h_{esh,n} + \sum_{m=1}^{N_{eg}} h_{hp,m} + \sum_{o=1}^{N_{eg}} h_{bo,o} + \sum_{k=1}^{N_{eg}} h_{hst,k} = \sum_{p=1}^{N_{loadh}} \Delta h_{load,p} \quad (2)$$

The heat load of the electric heat storage heater is not included in the following analysis. Therefore, $\sum_{n=1}^{N_{esh}} \Delta e_{esh,n} = 0$ in Eq. (1), and $\sum_{n=1}^{N_{esh}} h_{esh,n} = 0$ in Eq. (2).

4. Analysis Method

4.1 Setup of the Load

The electric power load and heat load of Syowa Base used in the analysis are based on the previous electric power load, as measured by Nishikawa et al. in a period between 2010 and 2011. Changes in the outside temperatures influence the electric power load; in addition, fluctuations in the electric power load from observation equipment, household appliances, and so forth cannot be expected. The electric power load of a representative day of every month is chosen at random from within the range of the minimum and the maximum past-record values for the electric power load of the same month. The electric power load $\Delta e_{load,month,t}$ of time t for each representative day of each representative month is calculated using Eq. (3). Here, θ is a random number between 0 and 1. The first term of the right-hand side adjusts the magnitude of the electric power load according to the difference of the target temperature (T_o), such as the room temperature of the base, and the temperature outside ($T_{\infty,t}$) at any given time t. The second term on the right-hand side describes fluctuations in the load ranging between the maximum ($\Delta e_{load,month,\max}$) and the minimum ($\Delta e_{load,month,\min}$) electric power load in the representative month. Figure 10 (a) shows an example computation for the electric power load according to Eq. (3).

$$\Delta e_{load,month,t} = \Delta e_{load,month,ave} \cdot \frac{24 \cdot \left(T_o - T_{\infty,t}\right)}{\sum_{t=1}^{24} \left(T_o - T_{\infty,t}\right)} + \left(\Delta e_{load,month,\max} - \Delta e_{load,month,\min}\right) \cdot \left(\theta - 0.5\right) \tag{3}$$

Equation (4) describes the heat load of the whole SBMG in sampling time t for a representative day of a representative month. The first term on the right-hand side of Eq. (4) is the adjustment of the heat load based on differences in the target temperatures and the outside temperature, while $\Delta h'_t$ refers to the past-record values of the past fuel consumption by both the boiler and the heater during heating in time t. The 2nd item on the right-hand side is a recorded value for the amount of exhaust heat from the engine generator. $\Delta h'_t$ and $h'_{eg,t}$ provide the past records through the measurement results of Nishikawa et al. [9] and others in 2010 to 2011, and the 51st party in 2009 to 2010 [1, 2]. An example of the heat load pattern calculated by Eq. (4) is shown in Fig. 10 (b).

$$\Delta h_{load,t} = \Delta h'_t \cdot \frac{\left(T_o - T_{\infty,t}\right)}{\sum_{t=1}^{24}\left(T_o - T_{\infty,t}\right)} + h'_{eg,t} \tag{4}$$

where,

$$h'_{eg,t} = 1.5486 \cdot \lambda_{eg,t} + 45.7368 \tag{5}$$

$\lambda_{eg,t}$ is a load factor of the engine generator at sampling time t, and the approximate expression in Eq. (5) was obtained from the measurement results by Nishikawa et al.

4.2 Equipment Characteristics

4.2.1 Engine Generator

As the main power supply of the SBMG, three sets of engine generators of 113 kW each are introduced (i = 1, 2, 3). An assumption is that the engine generator is a general-purpose item in Japan and that its power generation efficiency $\eta_{ege,i}$ is set, as in Eq. (6), from the engine load factor $\lambda_{eg,i}$ and the efficiency $\eta_{gt,i}$ [11]. Although the engine's maximum efficiency is 43.6%, the loss of the generator is set to 10% and the maximum power generation efficiency is set to 39.2%. Because actual heat dissipation losses and the performance heat exchangers are not known, a calculation of the amount of an engine generator's exhaust heat uses the overall efficiency of the present central power supply for a 240 kW engine generator. Figure 11 shows each efficiency for the 113 kW engine generator. The overall efficiency of the figure is set up similarly to the engine generator for the current central power supply. Therefore, the heating efficiency of the 113 kW engine generator is a value that excludes the power generation efficiency from the overall efficiency. Equation (7) is an approximate expression for the load factor of the engine generator and the heat power efficiency.

$$\eta_{ege,i} = \left(-0.00000356 \cdot \lambda_{eg,i}^2 + 0.001493 \cdot \lambda_{eg,i} + 0.3128\right) \cdot \eta_{gt,i} \tag{6}$$

$$\eta_{egh,i} = 0.001 \cdot \lambda_{eg,i}^2 - 0.2867 \cdot \lambda_{eg,i} + 41.60 \quad (7)$$

345

346 4.2.2 The Heat Pump

347 The heating medium that is heated by engine exhaust heat returns to an exhaust heat exchanger
348 after supplying heat to each heat demand–side site. Because the heat pump is introduced into the heat
349 medium mid-course, the heat source of the low-temperature heat pump is sufficiently higher than the
350 outside temperature. Therefore, the COP in this paper is set to 4.0. Moreover, the efficiency $\eta_{mt,i}$ of the
351 electric motor for the drive of the heat pump is set to 0.9. Heating power $Q_{w2,i,t}$ of the heat pump is
352 expressed with Eq. (8) from the energy flow shown in Fig. 9. Moreover, the COP of the heat pump is
353 defined by Eq. (9).

354

$$Q_{w2,i,t} = Q_{4,i,t} + L_{mt,i,t} = Q_{2,i,t} - Q_{w1,i,t} - Q_{loss,i,t} + P_{mt,i,t} \cdot \eta_{mt,i} \quad (8)$$

$$Q_{w2,i,t} \Big/ L_{mt,i,t} = COP \ (= 4.0) \quad (9)$$

355

356 4.2.3 Green Energy Equipment

357 Figure 12 shows the output characteristics of PV, with an 18% power generation efficiency based on
358 the amount of global solar radiation shown in Fig. 3 (c). Fig. 13 also shows the power performance
359 characteristics of the wind power system linked to the SBMG. Cut-in speed and cutout speed, assuming
360 the introduction of a wind power generator, are 5 m/s and 20 m/s, respectively, and the rated output is
361 10 kW at 12.5 m/s or more of wind velocity. Moreover, the power output e_{wp} of wind power generation
362 in the wind velocity range from the cut-in speed to the rated speed can be obtained from the
363 approximate expression (Eq. (10)) of the range of wind velocity falling between 5 m/s and 12.5 m/s, as
364 shown in Fig. 13.

365

$$e_{wp} = -0.000357 \cdot v_{wp}^4 + 0.0102 \cdot v_{wp}^3 - 0.00561 \cdot v_{wp}^2 - 0.1038 \cdot v_{wp} + 0.0612 \quad (10)$$

366

367 4.3 Analysis Procedure

The flow of the operation analysis of the SBMG is shown in Fig. 14. Parts (a) through (w) of the figure show each processing step. First, the meteorological data from Fig. 3 is input ((a)). Next, patterns of electric power load and heat load are calculated, in ((b) and (c)), according to Section 4.1, and the equipment characteristics of the power supply and the heat pump described in Section 4.2 are input in (d). From the equipment characteristics described in the upper part, Eq. (10), Fig. 12 and Fig. 13 are calculated for an output of PV and wind power generation for each given time of the representative day, to reference ((e) and (f)). For this analysis, both systems (e.g., the central power supply and the distributed power supply) are considered.

4-3-1 Analysis of the Central Power Supply System

The analysis flow for supplying electric power to the SBMG from one set of 240-kW diesel engine generators and for supplying heat from the exhaust heat pump and backup boiler is described below. The load factor and power generation efficiency (Eq. (6)) of the engine generator for each sampling time is calculated ((g)) using the electric power load. Next, based on the operation method of the system described in Fig. 8, the operating pattern of the engine generator and the storage of electricity and electric discharge are planned ((h)). For the operating pattern of the engine generator of every sampling time described above, the load factor and the power generation efficiency are calculated again ((i)). The amount of fuel consumption and exhaust heat (Fig. (b)) for each time of a given representative day are calculable ((j), (k)), given the power generation efficiency of the engine generator. Moreover, the heat output (Eq. (8)) of the heat pump, heat storage or heat output in the heat storage tank, and operation of the backup boiler is planned from the output pattern (Eq. (7)) of the exhaust heat ((l)). As a result, the fuel consumption of the boiler is calculable ((m)). The fuel consumption for each representative day is obtained by adding the fuel consumption of the engine generator to that of the backup boiler ((n)).

4-3-2 Distributed Power Supply System

The electric power is supplied to the SBMG from three sets of 113-kW diesel engine generators, and the supplying heat for the exhaust heat pump and backup boiler is described below. The load of each engine generator for every sampling time is decided from the power load ((o)). The load factor and power generation efficiency (Eq. (6)) for each engine generator are calculated by setting the load factor of each engine generator to 100 %, 50 %, or 0 % ((p)). Next, based on the operation method of the system

described in Fig. 8, the operating pattern of each engine generator and the electricity storage and discharge are planned ((q)). With respect to the operating pattern of each engine generator for every sampling time described above, the loading factor and the power generation efficiency are again calculated ((r)). From the power generation efficiency of each engine generator, the fuel consumption and the amount of exhaust heat (Fig. 11) for each period of the representative day are calculable ((s), (t)). From the power pattern of the exhaust heat (Eq. (7)) of each engine generator, the heat output of a heat pump (Eq. (8)), the thermal storage or heat output of a heat storage tank, and the operation of a backup boiler is planned ((u)). As a result, the fuel consumption of each boiler is calculable ((v)). Fuel consumption in a representative day is obtained by adding the fuel consumption of each engine generator to that of all backup boilers ((w)).

5. Analysis Results

5.1 Improvements in Power Generation Efficiency after the Introduction of Operation Planning

Syowa Base is in a special environment: there is no solar radiation in winter (July), the average wind velocity is small in winter and large in summer (January), and the heating demand is larger than the electricity demand. When the production of green energy-based electricity increases, the load of the linked engine generators will decrease. Therefore, the engine generator is operates at a partial load with low efficiency. The monthly load factor of the engine generator was investigated first. Figure 15 shows calculated load factors of each system when the 1000 m^2 PV and 10-kW wind power generator 10 sets are introduced into the SBMG. System A is the central power supply (the conventional operating system) without green energy, and System B is a system that uses green energy from System A. The heat supply is augmented with a boiler in System A and System B, without a heat pump. System C is the same as System B, with operation planning shown in Fig. 8 and a heat pump. System D and System E describe distributed power supply systems with a heat pump and with the operation plan shown in Fig. 8. Because there is no solar radiation in winter (Fig. 15 (b)), for each result in Fig. 15, the fluctuation in supply capability is based on wind power generation. In contrast, in summer (Fig. 15 (a)) and in mid-season (Fig. 15 (c)), fluctuations in the power supply by PV and wind generation are added to the transmission network. Because the fluctuations in green energy in January are large, as shown in Fig. 15 (a), the load factor of Systems B and D, without the operation planning, changes significantly. When the operation planning shown in Fig. 8 is introduced, System C and System E are as shown in

Figs. 15 (a) and (c), and the corresponding daytime load factor can be increased significantly. As a result, when operation planning is introduced to the power generation efficiency shown in Fig. 16, System B and D will improve as System C and E did. From the results of Figs. 15 and 16, the introduction of the operation planning described in this paper offers a good opportunity for improving the power generation efficiency of the system.

5.2 Operation of the Engine Exhaust Heat and the Backup Boiler

Given the extensive heat demand of the Syowa Base, the operation planning of the engine generator (exhaust heat), boiler, and heat pump largely influence the fuel consumption of the whole base. Figure 17 shows the analysis results for the engine exhaust heat and the boiler output of a central power supply (System A) without green energy and for a central power supply (System B) with green energy. Because a considerable amount of green energy is added to the power network for the operation of System B in January, the power of the engine generator is suppressed, especially in the daytime. Therefore, the engine exhaust heat of System B is smaller than that of System A. As a result, there is more boiler fuel in System B, except in the daytime, with many more PV outputs than System A. In contrast, the operation of System A and System B depends on differences in wind power generation in July when PV output cannot be obtained. Because the average wind velocity in July is the smallest of all months, as shown in Fig. 17 (b), System A, the engine exhaust heat of System B, and the difference in the operation of the boiler are all small. As shown in Fig. 17 (b), the differences in the operation of the engine exhaust heat and the heat output of the boiler of System A and System B are also small.

Figure 18 shows the analysis results for the engine exhaust heat, heat pump output, the output of a backup boiler with green energy, a heat pump with a central power supply (System C), and the distributed power supply system (System D), with the associated operation planning shown in Fig. 8. In this case, the exhaust heat is frequently generated via partial load operation with a low power generation efficiency, as in System D in System C. As a result, the heat demand is fulfilled by shifting the time and by using the exhaust heat and heat output of the heat pump with the heat storage tank from System C. Therefore, System C does not require a backup boiler. System D corresponds to fluctuations in green energy and loading with two sets of engine generators. Because each engine generator is operated with a load factor (0%, 50%, or 100%), thermal power can result in large fluctuations. As shown in Figs. 18 and 17, because the load factor of the engine generator falls with the

power of daytime PV, the power from exhaust heat is minimal. In contrast, if a. Operating an engine generator with a high load for a short time and accumulating an electricity surplus power and b. Enough electricity is obtained, then the engine power will be dropped to a neutral level (0% of load factor) and power will be supplied from a battery, c. If the battery electricity level falls, the engine generator will be operated with a highly efficient full load, from a. to c., as shown in System D of Fig. 18 (b).

5.3 Fuel Consumption of the Backup Boiler and its Thermal Storage Characteristics

Figure 19 shows the analysis results of the monthly fuel consumption of the backup boiler. Because System A without green energy does not have additional energy (PV and wind power) unlike the other systems, it requires the most fuel consumption from its backup boiler. Next, there is a considerable amount of fuel consumption in the backup boiler in the central power supply system (System B) with green energy. Because a heat pump and the central power supply system (System C) with the operation planning described in Fig. 8 has many sources of heat power, a backup boiler is not needed in System C. Operating times with low engine generator loads are accomplished with the introduction of green energy in System B. As a result, there is little exhaust heat and fuel consumption in the backup boiler in System B. In contrast because System C provides enough green energy, the power of the heat pump is large. Therefore, installation of the backup boiler is not needed.

Figure 20 shows the results of the operation analysis for the heat storage tank. There is significant thermal storage at 24:00 in any month within System C. Therefore, heat exceeding the demand of the present Syowa Base is obtained using the heat pump. Surplus heat will be present in the January heat supply with a lot of PV power in System D. There is no surplus heat supply for System B. The operation planning is made so that the surplus exhaust heat and the surplus power may be stored with heat via the central power supply system (System C) with green energy. As a result, because the heat power of the heat pump will exceed the heat demand when green energy is fully supplied, the amount of thermal storage will increase with time, as shown in Fig. 20.

5.4 The Relationship between the Introduced Green Energy and Fuel Consumption

Figure 21 shows the analysis results of the fuel consumption of the distributed power supply system for a representative day every month when changing the area of the solar cell; the number of installed

aerogenerators are shown in Fig. 13. The distributed power supply system of Fig. 21 is linked with green energy and is introduced into the operation planning for Fig. 8 and the heat pump. The greatest fuel consumption occurs in July without PV power. In contrast, the fuel consumption of the system will decrease in January and October because of the large supply of PV power and the installation of many aerogenerators. Although wind power is the only source of green energy in July, the average wind velocity in July is lower than that of other months (78% to October, 74% to January). Therefore, the influence of changing the number of aerogenerators is small, as in Fig. 21 (b). When more green energy equipment is installed, the stability of the power supply for the overall power network will become a significant problem, but the SBMG is examining two measures at present. The first, which relates to load, can be controlled using the number of distributed engine generators required. The second, which relates to fluctuations in green energy, is suppressed with the introduction of an electric storage heater to each building, as shown in Figs. 2 and 7. For each of the two methods described above, the power quality (voltage, frequency, waveform) needs to be checked via a numerical simulation of the electrical power system.

Figure 22 shows the rate of fuel consumption for the distributed power supply system compared with the fuel consumption for the central power supply system with operation planning and green energy. For conditions with less fuel consumption in the distributed power supply system than in the central power supply system, the rate is less than 100% on each representative day, as shown in Fig. 22. When the installation of aerogenerators and the area of PV is small, the distributed power supply system is disadvantageous, as shown in Fig. 22 (a). Therefore, most differences between the central power supply system and the distributed power supply system will not be seen in July. A distributed power supply system is advantageous when a large number of unstable green energy units are introduced and when the load change is large. Therefore, as the green energy to the Syowa Base increases in future years, a corresponding fuel reduction (via the introduction of the distributed power supply system) can be expected.

5.5 Reduction in Fuel Consumption

Figure 23 shows the results of the calculated rate of fuel consumption for the proposed power supply system distribution (with the operation planning, green energy, and heat pump) to the central power supply system without green energy and to the current operation of Syowa Base. Because the

518 heat-to-power ratio for Syowa Base exceeds 1.0, operation of the heat power output control is
519 appropriate for the conventional central power supply system. In contrast, when there is no power
520 supply from green energy, the load of the engine generators increases for the operation of the heat
521 pump in the proposed power supply system distribution. As a result, the fuel consumption of the engine
522 generators increases. Therefore, as shown in Fig. 23 (a), the proposed power supply system distribution
523 of the area with few PV and wind power installations has disadvantages in terms of its fuel
524 consumption compared with the conventional central power supply system. However, when enough
525 green energy is obtained, significant fuel reductions from the conventional system are expected.
526
527 6. Conclusions
528 The amount of fuel transported from Japan is increasing every year as research and observation
529 progresses at the Antarctic Syowa Base. Although the observatory ship Shirase transports fuel to
530 Syowa Base from Japan once per year, reservation of cargo space for energy is a problem. Accordingly,
531 this research considered the construction of a small-scale energy network (Syowa Base Micro-Grid:
532 SBMG). Promotion of green energy utilization was investigated by updating the main power supply of
533 Syowa Base from a conventional central power supply system to a distributed power supply system. By
534 increasing the number of engine generators, operation planning of the charge and discharge of electric
535 power, and the exhaust heat pump, improvements in the load factor and the power generation
536 efficiency of the distributed engine generator linked to unstable green energy were evaluated. The
537 reduction of fuel consumption in the proposed system was investigated by numerical analysis, leading
538 to the following conclusions.
539 (1) Because PV generates significant energy, the loading factor for the engine generators using a central
540 power supply system as the main power supply falls sharply from 7:00 to 16:00 between summer
541 (January) and mid-season (October). Therefore, the minimum load factor of the engine generator was
542 set to 50%, and operation was planned such that the load factor of the engine generator might be
543 maintained with the charge and discharge of a battery. As a result, the load factors and power
544 generation efficiency of both the central power supply system and the distributed power supply system
545 are improved when compared with the conventional method.
546 (2) When the green energy power supply increases, the load of the engine generator will decrease. As a
547 result, because the amount of engine exhaust heat falls, the fuel consumption of the boiler must

548 increase to satisfy the heat load. Accordingly, in this research, the increase in the load factor and the
549 power generation efficiency of the engine generator based on the introduction of an electric heat pump
550 was planned. Based on these results, the relationship between the introduction of green energy and
551 fuel consumption was clarified.
552 (3) Most differences in the fuel consumption of the central power supply system and the distributed
553 power supply system are not seen in winter (July) without PV power. The distributed power supply
554 system is advantageous when the introduction of unstable green energy causes large power load
555 fluctuations. Therefore, when the green energy levels of Syowa Base are increased in the future, the
556 distributed power supply system will likely reduce the fuel consumption.
557 (4) When the area of PV is large and many aerogenerators are introduced, the fuel consumption of the
558 energy system with the distributed power supply system will decrease. Only wind power can be used as
559 green energy in winter (July), and the average wind velocity in winter is low compared with other
560 months. Therefore, the reduction in fuel consumption during winter by the installation of
561 aerogenerators is small compared with that of other months.
562 (5) When there are few areas covered by PV and the installation of wind power is minimal, the
563 proposed power supply system distribution may be disadvantageous compared with the conventional
564 central power supply system. Little green energy can be provided and fluctuations in the supply occur,
565 and if the load factor of the engine generator can be maintained at a fixed energy level, then the central
566 power supply system would be more advantageous than the distributed power supply system.
567

568 **Acknowledgments**

569 The authors wish to thank the National Institute of Polar Research in Japan for their partial support
570 of this research.
571

572 **Nomenclature**

N	:	A number
e	:	Electric power [kW]
e_{pst}	:	Power load of Syowa base [kW]
Δe	:	Consumption of electric power [kW]

h : Heat [kW]

$h_1 - h_5$: Heat (See Fig. 9) [kW]

h_{w1}, h_{w2} : Heat of hot water (See Fig. 9) [kW]

h'_{eg} : Record of past engine exhaust heat [kW]

Δh : Consumption of heat [kW]

$\Delta h'$: Fuel consumption of the boiler and heater for space heating [kW]

l : External work [kW]

T_o : Target temperature [K]

T_∞ : Outside temperature [K]

t : Sampling time [Hour]

Greek characters

η : Efficiency

η_{ege} : Power generation efficiency

η_{egh} : Heat output efficiency

λ : Load factor [%]

v : Wind speed [m/s]

θ : Random number between 0 and 1

Subscript

ave : Average

bo : Boiler

bt : Battery

eg : Engine

esh : Electric heat storage heater

gt : Generator

hp : Heat pump

hst : Heat storage tank

load : Load

loss : Loss

mt : Electric motor of heat pump

pv	:	Photovoltaics
pvu	:	Unit of photovoltaics
wg	:	Wind power generator
wpu	:	Unit of wind power generator

573

574 **References**

575 [1] Nishikawa S, Abiko H, Kurihara J, Ishizawa K, Endo N. Fundamental study for introduction of
576 renewable energy into Syowa base, IEEJ transactions on power and energy, Transactions of IEE Japan
577 2011;131(9);778-785. (in Japanese)
578 [2] National Institute of Polar Research Japan. Present condition of the energy equipment of Syowa
579 base, The 1st South Pole green energy use examination WG 2011;4-30.
580 [3] Manfren M, Caputo P, Costa G. Paradigm shift in urban energy systems through distributed
581 generation: Methods and models, Applied Energy 2011;88(4);1032-1048.
582 [4] Ren H, Zhou W, Nakagami K, Gao W, Wu Q. Multi-objective optimization for the operation of
583 distributed energy systems considering economic and environmental aspects, Applied Energy
584 2010;87(12);3642-3651.
585 [5] Bakos G C. Distributed power generation: A case study of small scale PV power plant in Greece,
586 Applied Energy 2009;86(9);1757-1766.
587 [6] Blarke M B. Towards an intermittency-friendly energy system: Comparing electric boilers and heat
588 pumps in distributed cogeneration, Applied Energy 2012;91(1); 349-365.
589 [7] Ruan Y, Liu Q, Zhou W, Firestone R, Gao W, Watanabe T. Optimal option of distributed generation
590 technologies for various commercial buildings, Applied Energy 2009;86(9);1641-1653.
591 [8] Mancarella P, Chicco G. Global and local emission impact assessment of distributed cogeneration
592 systems with partial-load models, Applied Energy 2009;86(10);2096-2106.
593 [9] National Institute of Polar Research Japan. Present condition of the energy equipment of Syowa
594 base, The 2nd South Pole green energy use examination WG 2011;1-66.
595 [10] Homepage of Japan Metrological Agency. http://www.data.jma.go.jp/obd/stats/etrn/index.php;2012.
596 [11] Homepage of Denyo Co., Ltd. http://www.denyo.co.jp/english/index.html;2012.

597

598

599 **Captions**

600 Fig. 1 Configuration of the conventional electric power networks and heating systems at Syowa
601 station

602 Fig. 2 Configuration of the future proposed distribution model for the power network of Syowa station

603 (a) Electric power network and heating system

604 (b) Heating system A

605 (c) Heating system B

606 Fig. 3 Meteorological data at Syowa base

607 (a) Average monthly outdoor air temperature

608 (b) Average monthly wind velocity

609 (c) Global solar radiation

610 Fig. 4 Monthly electric power consumption of the 51st party (2009-2010)

611 (a) Electric power load

612 (b) Monthly power supply

613 Fig. 5 Monthly heat demand of the 51st party (2009-2010)

614 Fig. 6 Performance of the engine generator of a central system and a distributed system

615 (a) Example of fuel consumption for a central and distributed power supply

616 (b) Characteristics of the engine generators, assuming introduction

617 Fig. 7 The proposed microgrid

618 Fig. 8 The proposed operation planning

619 (a) Electric power demand

620 (b) Output of electric power of green energy

621 (c) Operating pattern of the engine generators calculated from the power balance

622 (d) Operation planning of the engine generators and the battery

623 (e) Results of the operation plan for each engine generator

624 Fig. 9 Energy flow

625 Fig. 10 Power demand models

626 (a) Electric power demand

627 (b) Heat demand

628 Fig. 11 Efficiency characteristics of the 113 kW engine generator installed in the SBMG

629 Fig. 12 Performance of photovoltaics

630 Fig. 13 Power performance of the wind power generator

631 Fig. 14 Analysis flow

632 Fig. 15 Results of load factors (1000 m^2 PV, 10 kW wind power generators, 10 sets)

633 Fig. 16 Results of power generation efficiency (1000 m^2 PV, 10 kW wind power generators, 10 sets)

634 Fig. 17 Output of exhaust and boiler heat from the central power supply (1000 m^2 PV, 10 kW wind
635 power generators, 10 sets)

636 Fig. 18 Output of exhaust, heat pump and back-up boiler heat from power system with green energy
637 (1000 m^2 PV, 10 kW wind power generators, 10 sets)

638 Fig. 19 Fuel consumption of backup boiler (1000 m^2 PV, 10 kW wind power generators, 10 sets)

639 Fig. 20 Results of operation planning with heat storage (1000 m^2 PV, 10 kW wind power generators,
640 10 sets)

641 Fig. 21 Results of fuel consumption for the proposed power supply distribution with the heat pump

642 Fig. 22 Rate of fuel consumption of the distributed power supply with the heat pump to the central
643 power supply with a back-up boiler

644 Fig. 23 Rate of fuel consumption for the proposed power supply distribution with the heat pump
645 connected to the conventional central power supply with the boiler

646

647 Table 1 Annual consumption of fuel

648

649

650

651

Fig. 1 Configurations of conventional electric power network and heating system at Syowa station

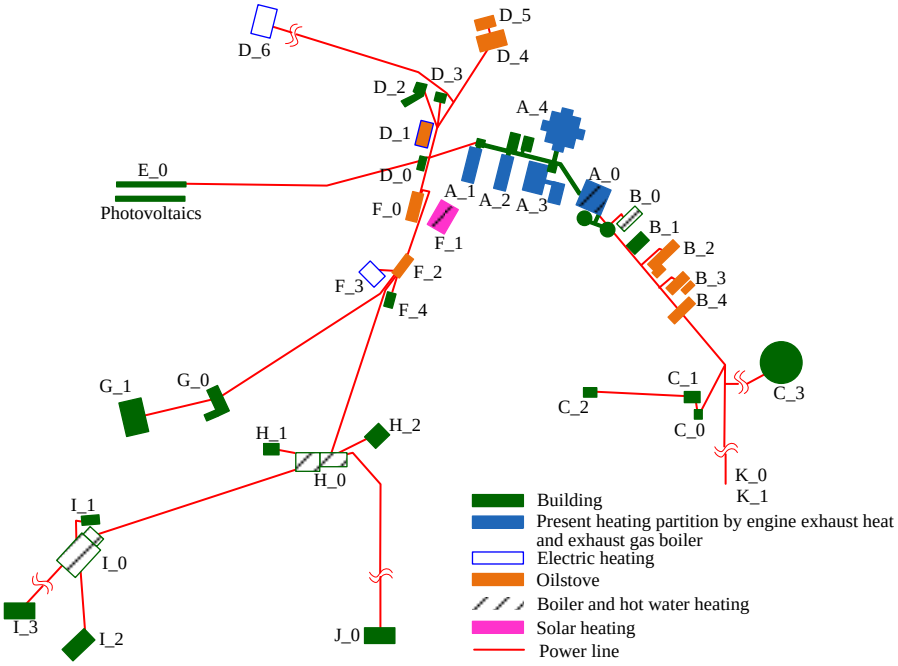

Fig. 2 Configurations of future proposal model of a distributed power network of Syowa station

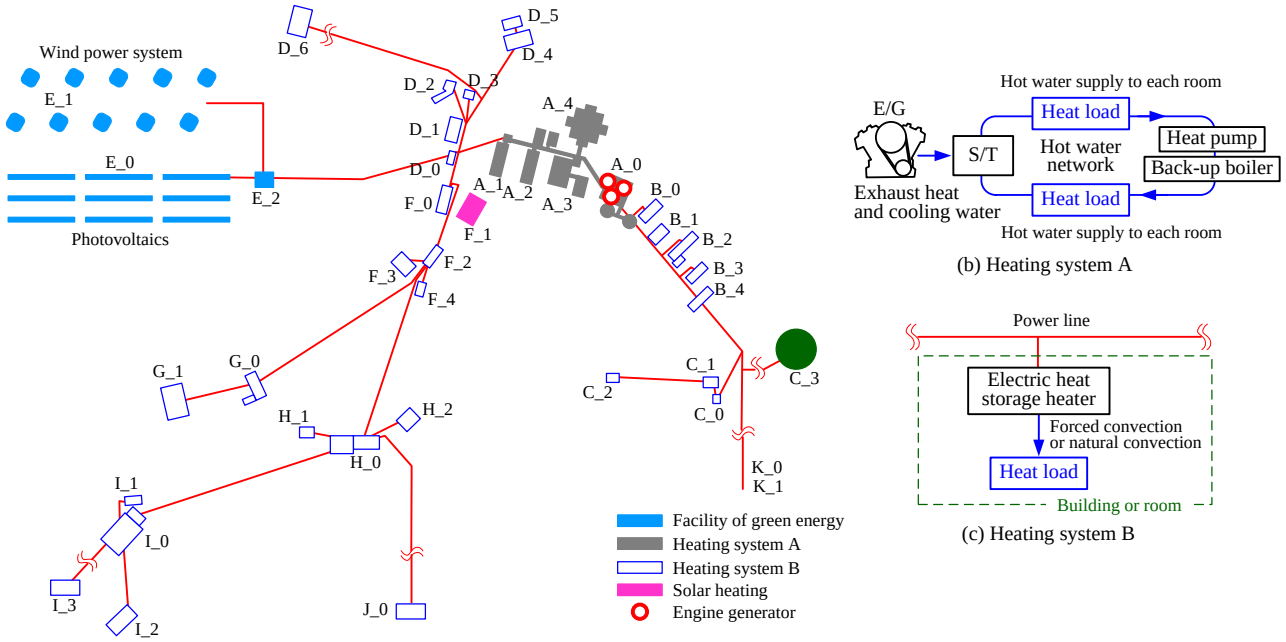

(a) Electric power network and heating system

(b) Heating system A

(c) Heating system B

690 Fig. 3 Meteorological data at Showa base

691

692

693

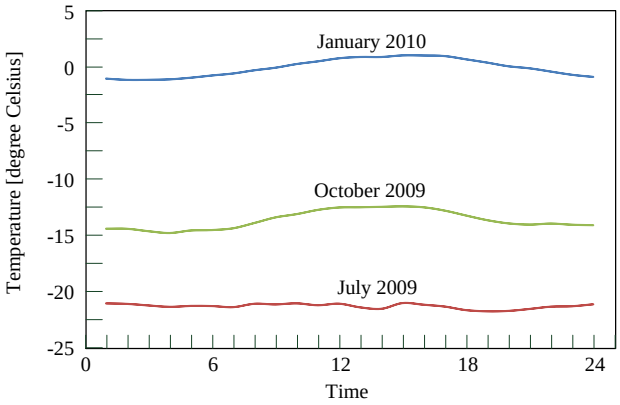

(a) Outdoor air temperature of monthly average

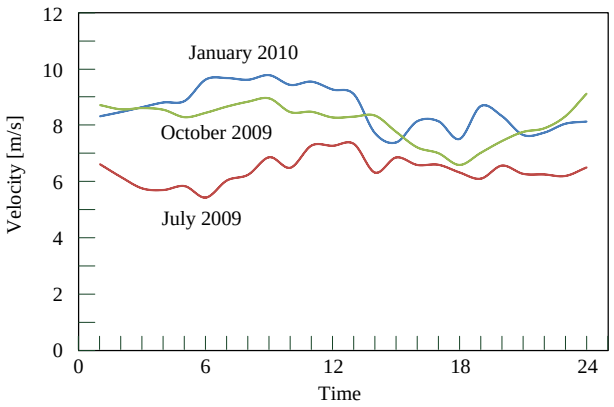

(b) Wind velocity of monthly average

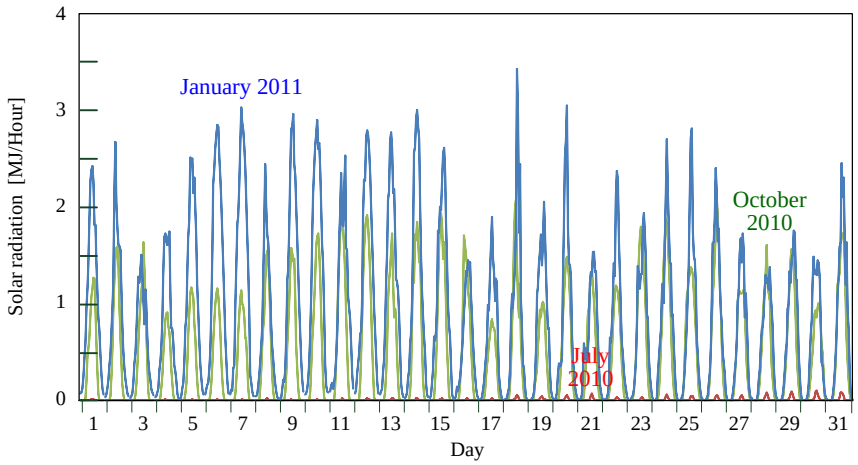

(c) Global solar radiation

694

695

696

697

698

699

700

701

702

703

Fig. 4 Monthly electric power consumption of the 51st party (2009-2010)

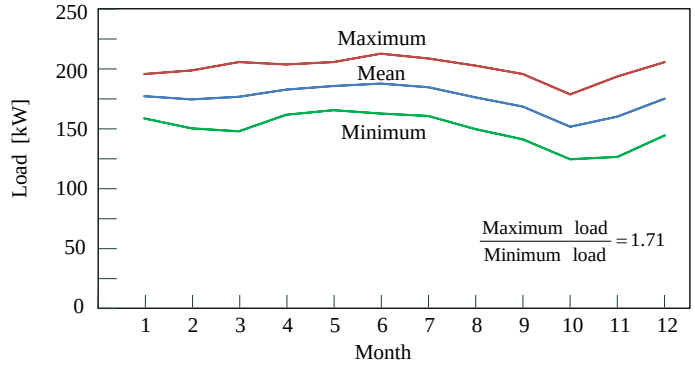

(a) Electric power load

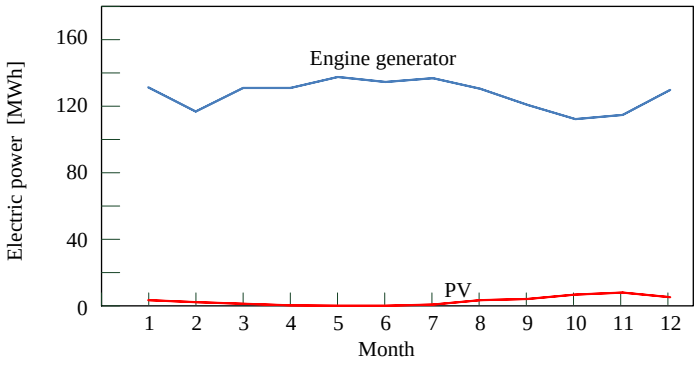

(b) Monthly power supply

Fig. 5 Heat demand amount of every month of the 51st party (2009-2010)

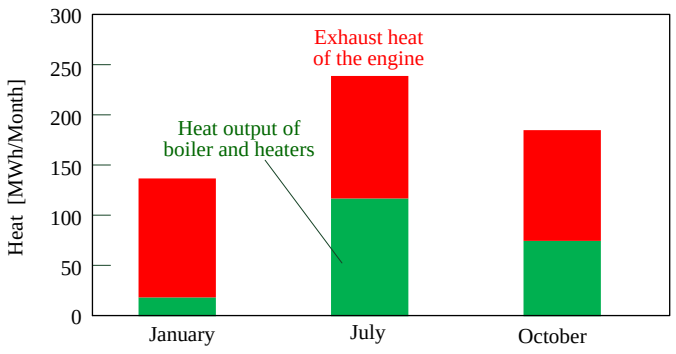

Fig. 6 Performance of engine generator of a central system and a distributed system

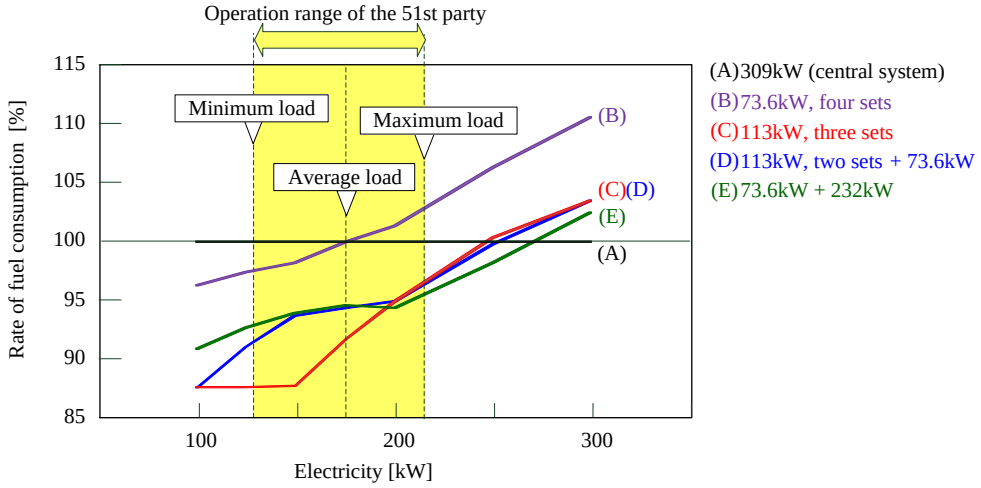

(a) Example of the fuel consumption of a central and distributed power supply

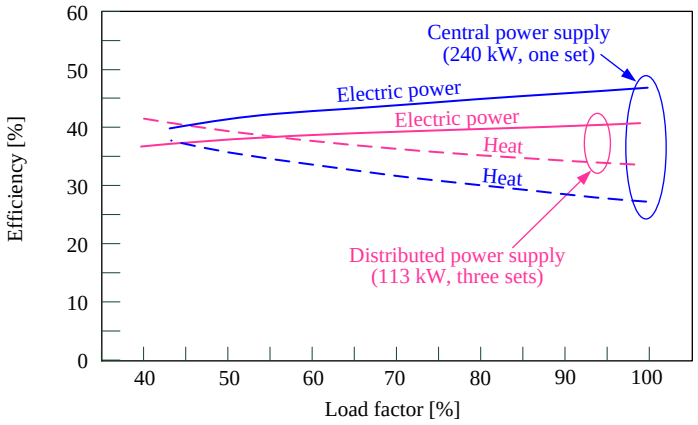

(b) Characteristics of the engine generators assuming introduction

Fig. 7 The proposed microgrid

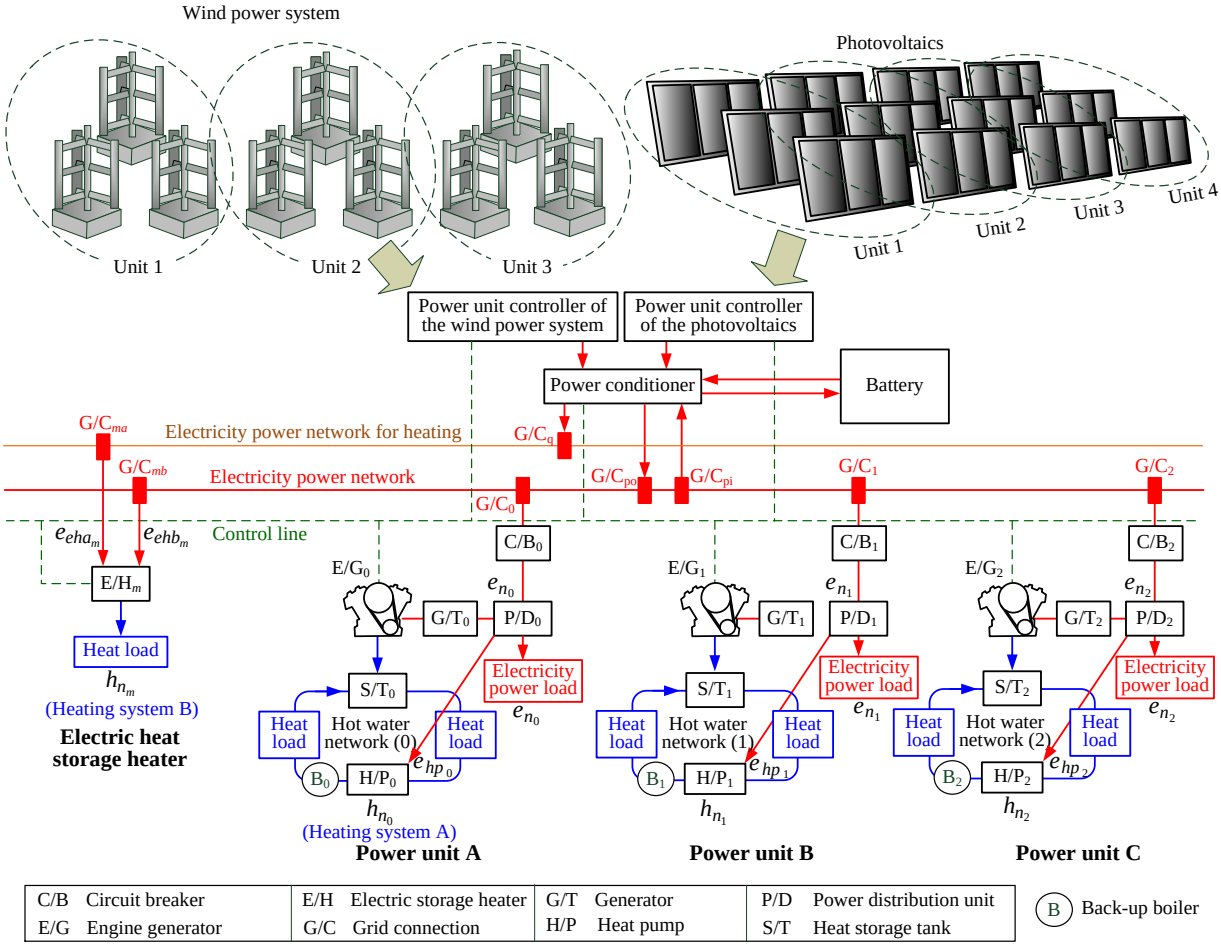

Fig. 8 Proposed operation planning

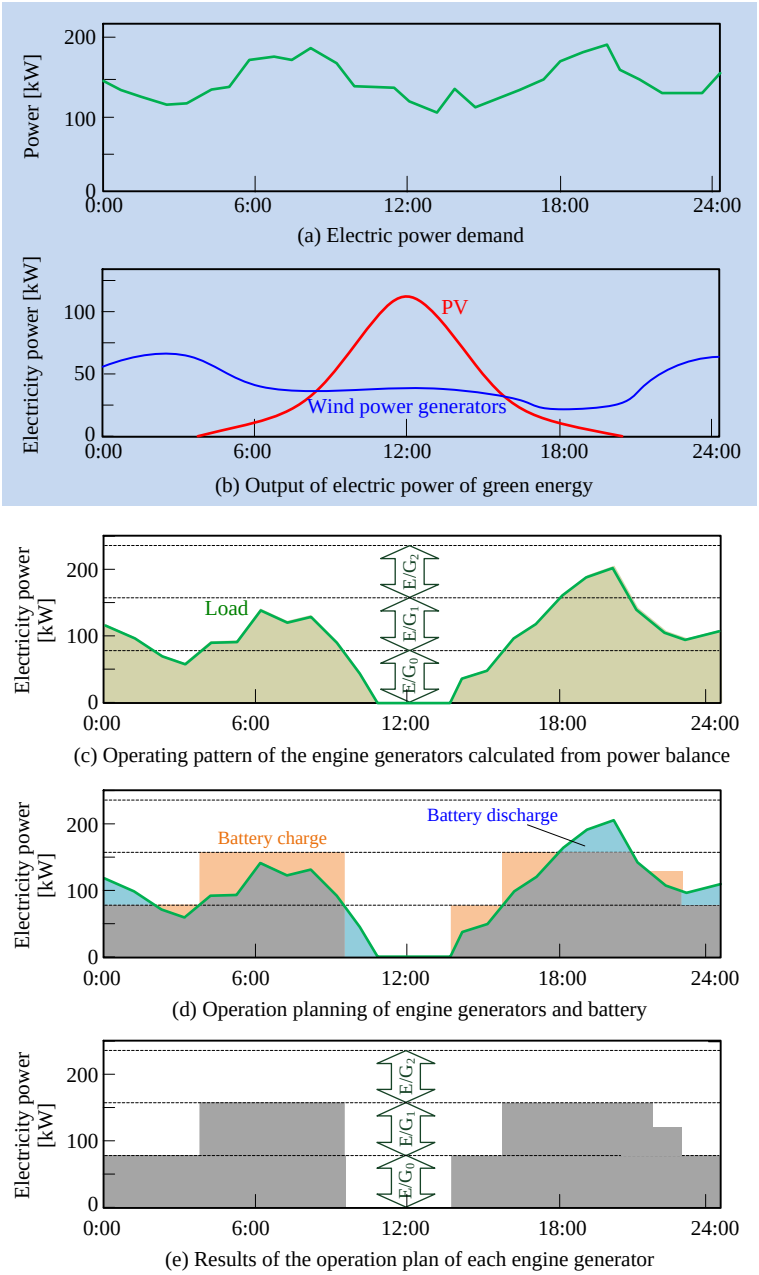

749 Fig. 9 Energy flow

750

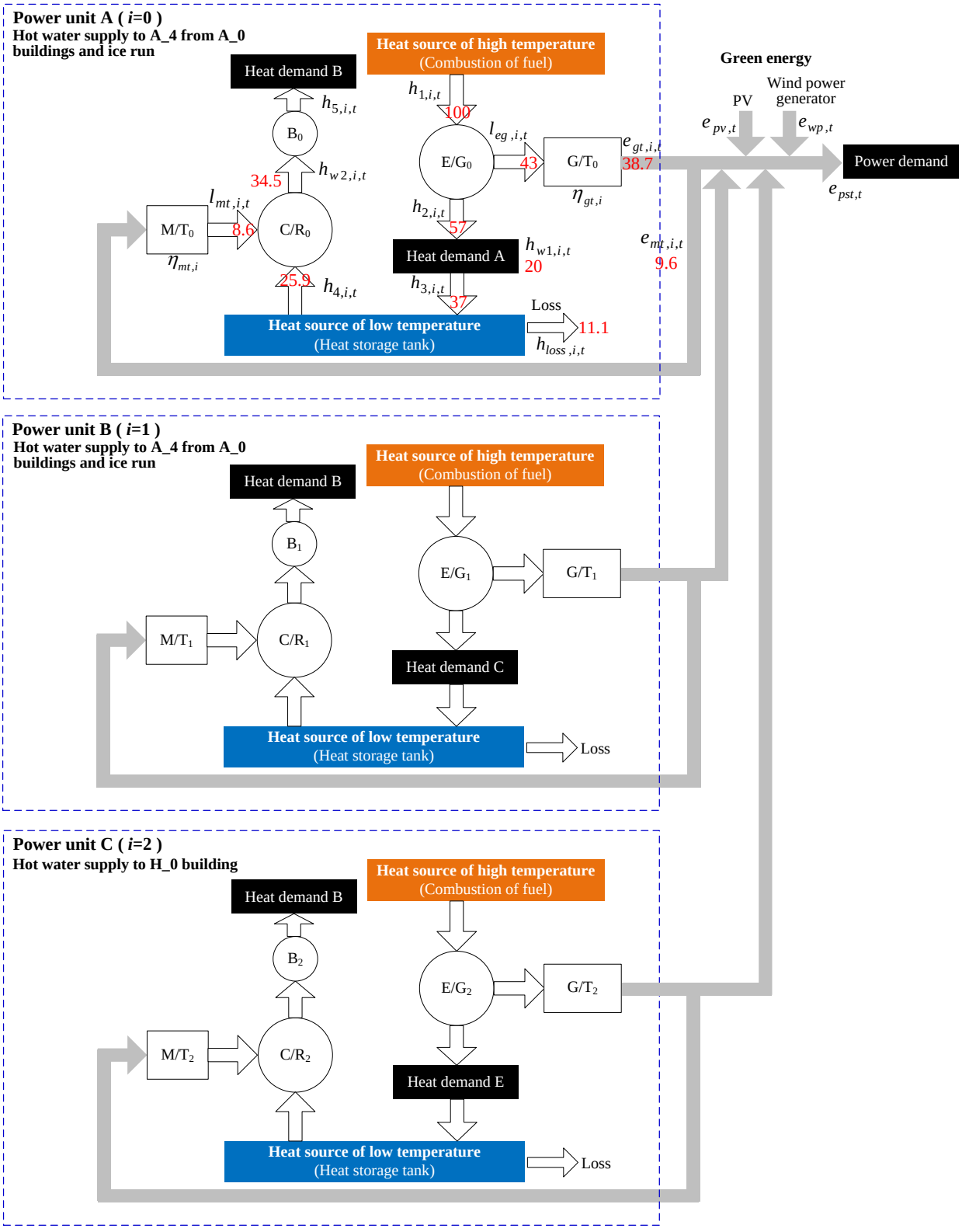

751

752

753 Fig. 10 Power demand models

754

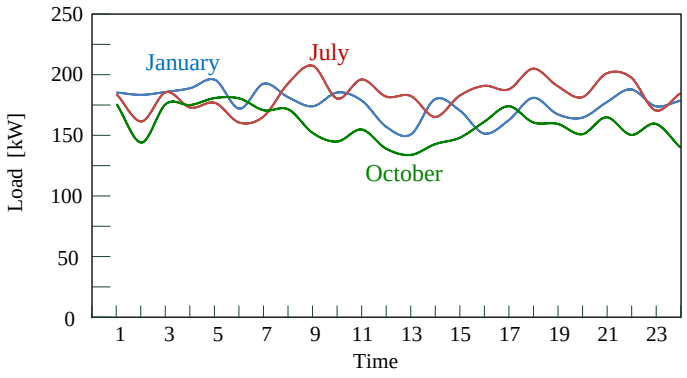

(a) Electric power demand

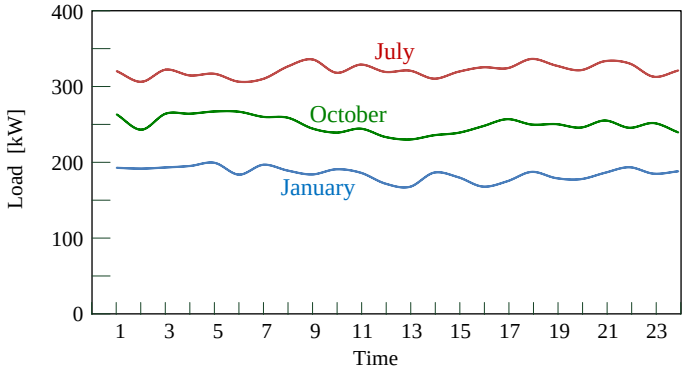

(b) Heat demand

755

756

757

758 Fig. 11 Efficiency characteristics of 113 kW engine generator installed in the SBMG

759

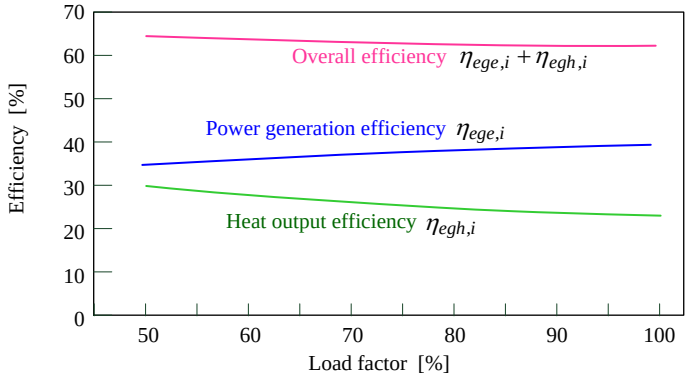

760

761

Fig. 12 Performance of photovoltaics

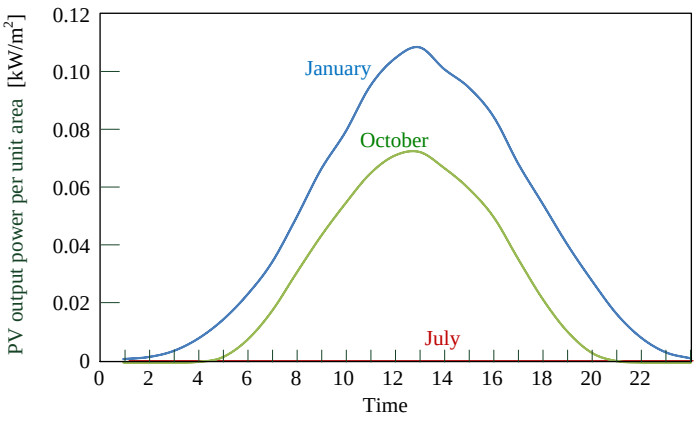

Fig. 13 Power performance of wind power generator

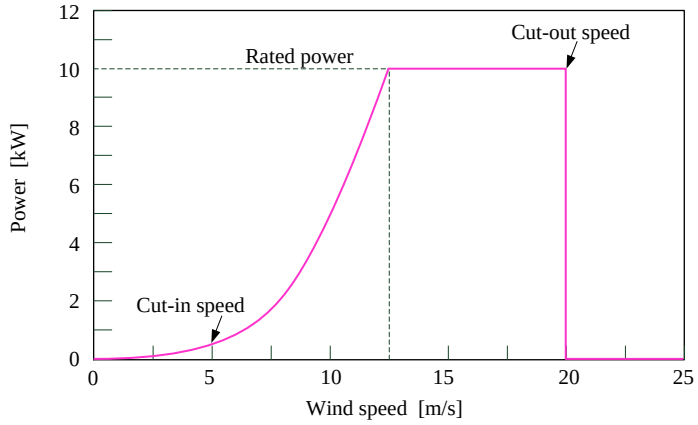

Fig. 14 Analysis flow

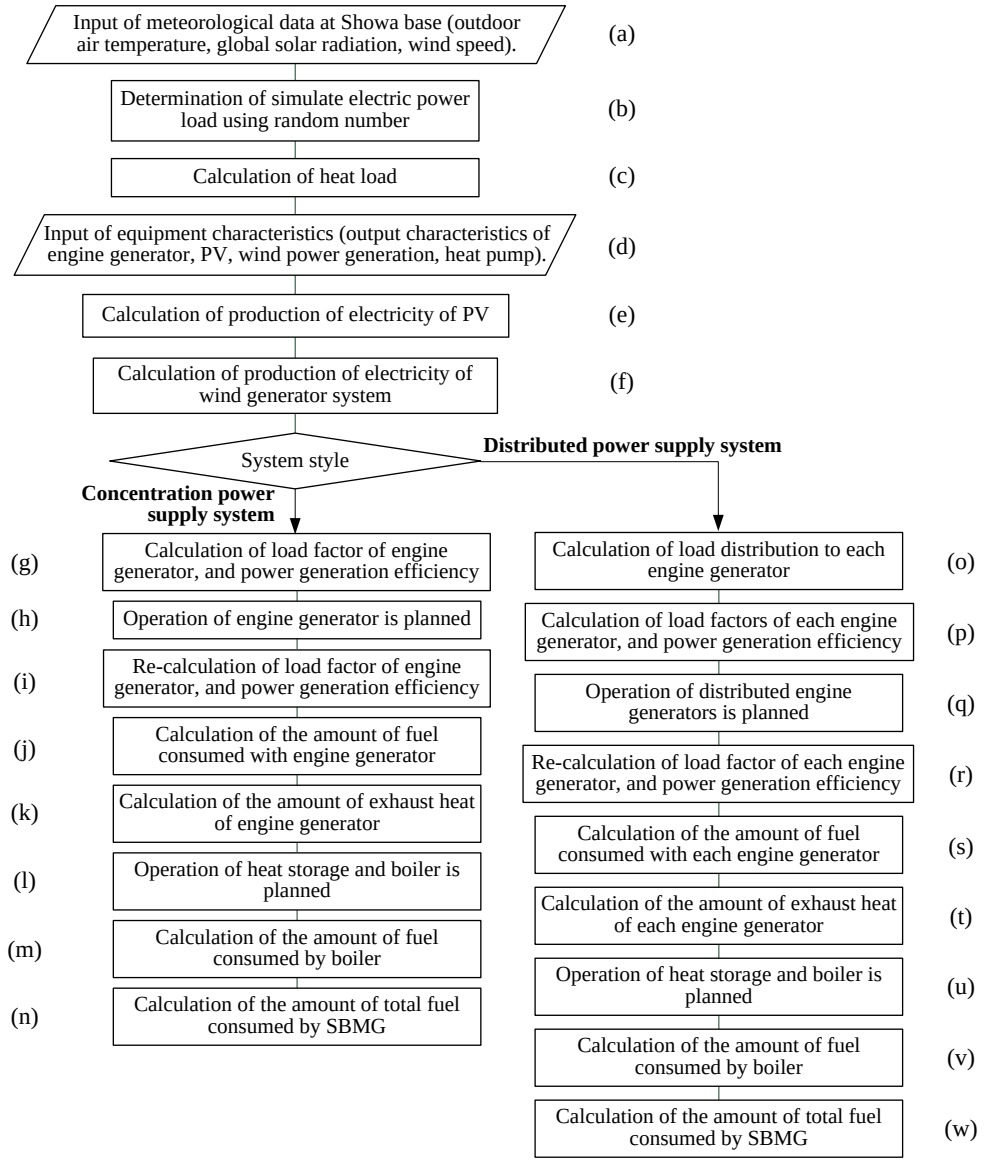

788 Fig. 15 Results of load factors (1000 m2 PV, 10 kW wind power generators 10 sets)

789

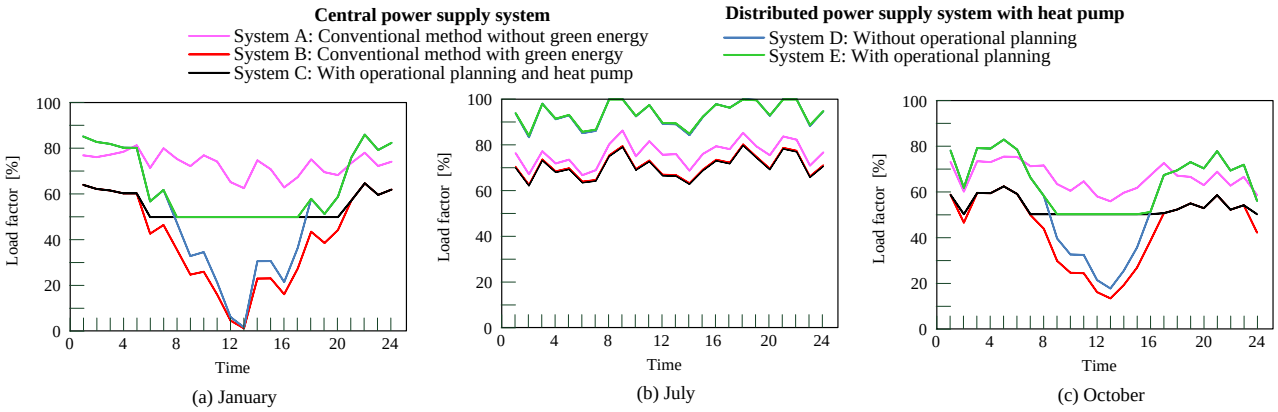

790

791 Fig. 16 Results of power generation efficiency (1000 m^2 PV, 10 kW wind power generators 10 sets)

792

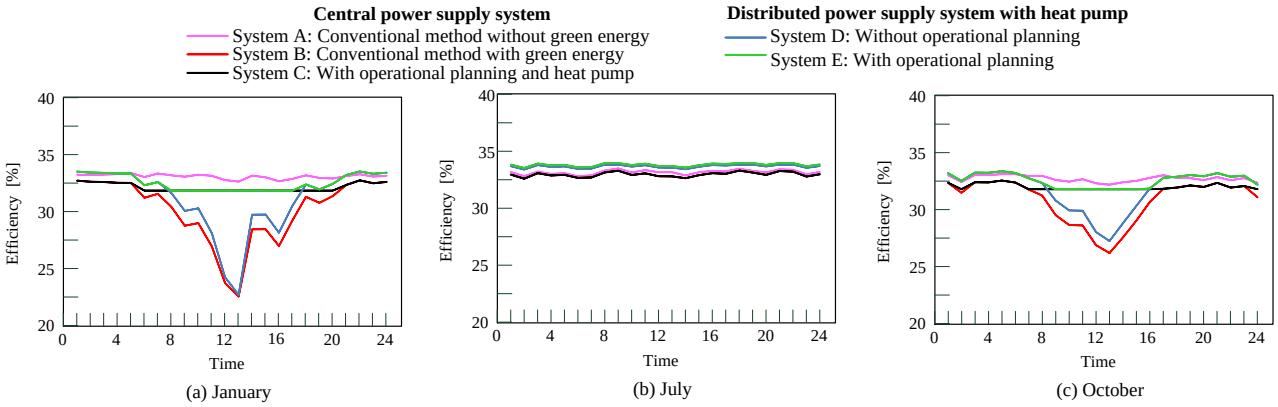

793

794 Fig. 17 Output of exhaust heat and boiler from central power supply (1000 m^2 PV, 10 kW wind power generators

795 10 sets)

796

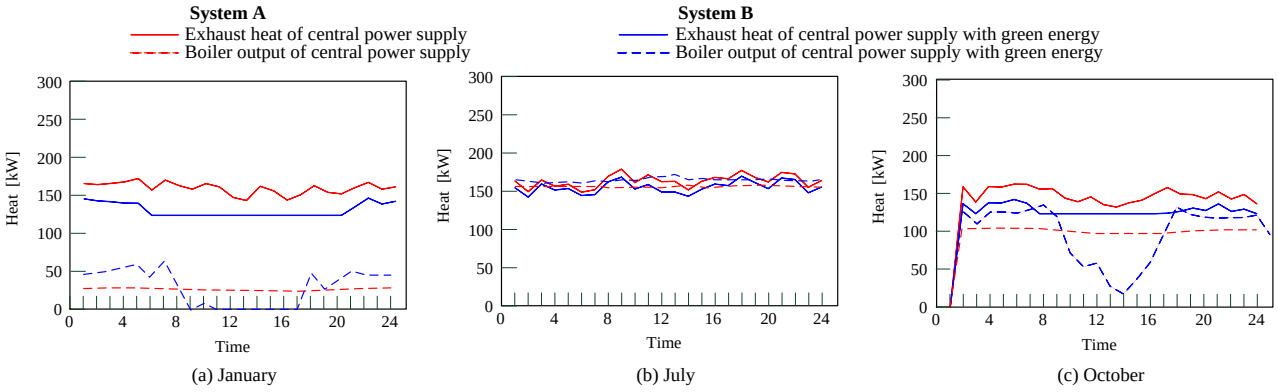

797

Fig. 18 Output of exhaust heat, heat pump and back-up boiler from power system with green energy (1000 m2 PV, 10 kW wind power generators 10 sets)

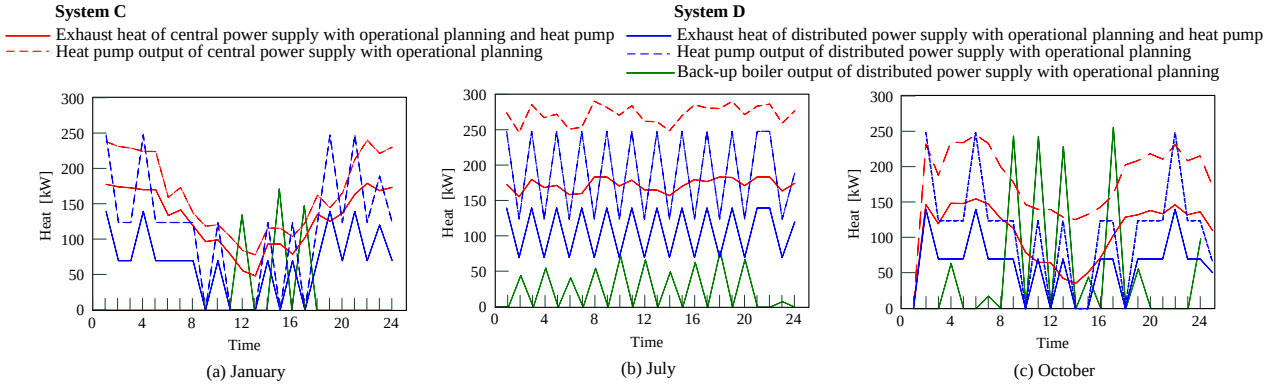

Fig. 19 Fuel consumption of backup boiler (1000 m2 PV, 10 kW wind power generators 10 sets)

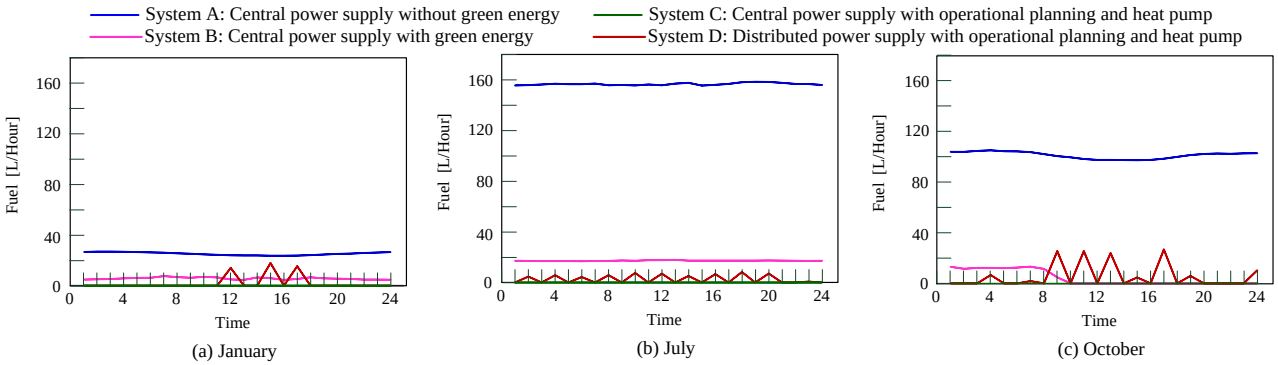

Fig. 20 Results of operation planning of heat storage (1000 m2 PV, 10 kW wind power generators 10 sets)

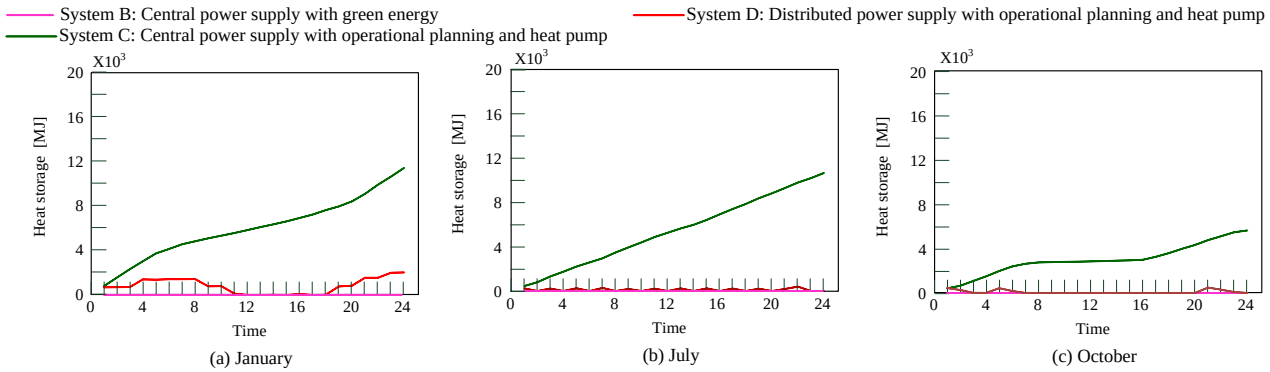

Fig. 21 Results of fuel consumption of the proposed distributed power supply with heat pump

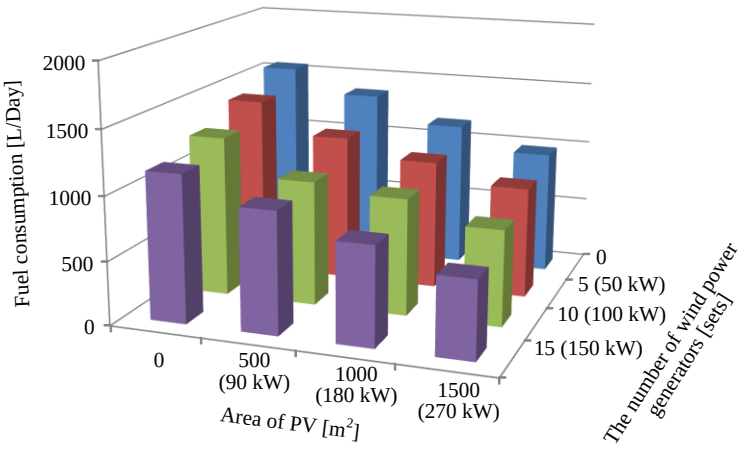

(a) January

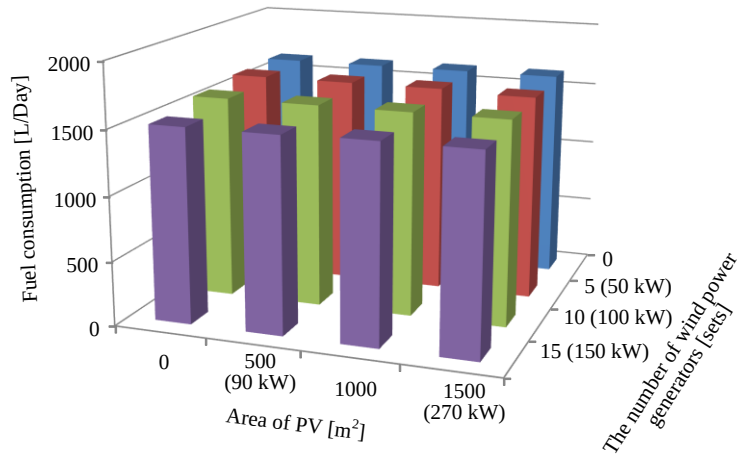

(b) July

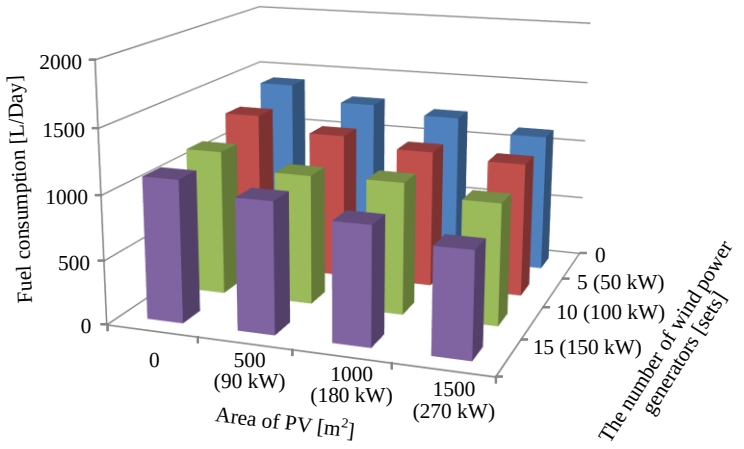

(c) October

Fig. 22 Rate of fuel consumption of distributed power supply with heat pump to central power supply with back-up boiler

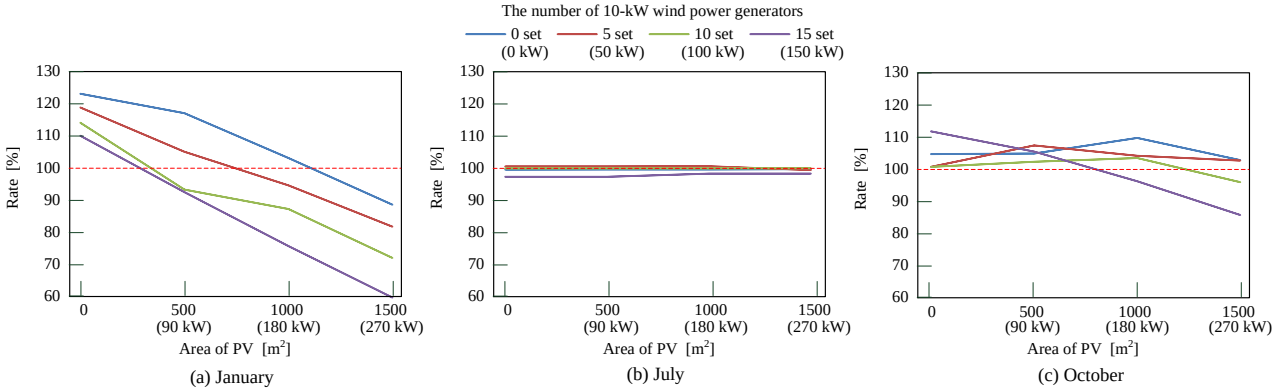

Fig. 23 Rate of fuel consumption of proposal distributed power supply with heat pump to conventional central power supply with boiler

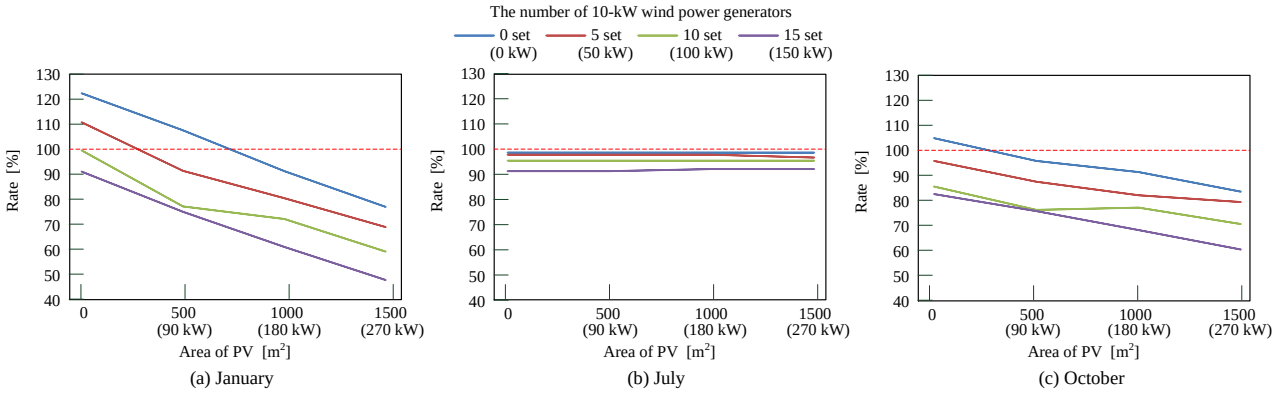

Table 1 Annual consumption of fuel

Fuel for power generation	JIS K 2204 (diesel)	430 kL
Fuel for boiler and heaters	JP-5 (jet fuel)	87 kL
Other		90 kL